Corrosion - inhibiting properties of molybdenum - containing pigments in coatings

Tereza Hájková and Andrea Kalendová*
Faculty of Chemical Technology, University of Pardubice, 532 10 Pardubice, Czech Republic

Abstract

Purpose - Synthesise anticorrosion pigments containing molybdenum for paints intended for corrosion protection of metals.

Design/methodology/approach - The anticorrosion pigments were prepared by high-temperature solid-state synthesis from the appropriate oxides, carbonates, and calcium metasilicate. Stoichiometric molybdates and core-shell molybdates with a non-isometric particle shape containing Ca, Sr, Zn, Mg, and Fe were synthesised. The pigments were examined by X-ray diffraction analysis and by scanning electron microscopy. Paints based on an epoxy resin and containing the substances at a pigment volume concentration (PVC) = 10 vol.% were prepared. The paints were subjected to physico-mechanical tests and to tests in corrosion atmospheres. The corrosion test results were compared to those of the paint with a commercial pigment, which is used in many industrial applications.

Findings - The molybdate structure of each pigment prepared was elucidated. The core-shell molybdates exhibit a non-isometric particle shape. The pigments prepared were found to impart a very good anticorrosion efficiency to the paints. A high anticorrosion efficiency was found with the pigments $Fe_2(MoO_4)_3$ and $Fe_2(MoO_4)_3$**/**$CaSiO_3$ and with Mg and Zn molybdates.

Practical implications - The pigments can be used for the formulation of paints intended for the corrosion protection of metals. The pigments also improve the paints´ physical properties.

Originality/value - The use of the pigments in anticorrosion paints for the protection of metals is new. The benefits include the use and the procedure of synthesis of the anticorrosion pigments which are free from heavy metals and are acceptable from the aspect of environmental protection. Moreover, the core-shell molybdates, whose high efficiency is comparable to that of the stoichiometric molybdates, have lower molybdenum contents.

Key words Organic coating, Paint, Core-shell pigment, Anticorrosion pigment, Molybdate, Wollastonite, Non-isometric particles

Paper type Research type

1. Introduction

Zinc phosphate is currently the most frequently used pigment for anticorrosion paints (Attar and Naderi, 2009; Bethencourt *et al.,* 2003; Gnot and Zubielewicz, 2004). Although highly efficient (Attar and Naderi*,* 2009; Deya *et al.,* 2002), conventional pigments containing lead or hexavalent chromium are unsuitable from the point of view of environmental protection (Amo *et al.,* 2002; Attar and Naderi, 2009; Blustein *et al.,* 2005). The development of nontoxic anticorrosion pigments capable of replacing chromate pigments is certainly not finished yet (Attar and Mahdavian, 2005). Molybdate - based pigments seem to be a promising solution for the protection of metals using coating materials. Molybdate-based pigments were first manufactured in the United States.

It is an asset of anticorrosion pigments with molybdenum that the molybdate anion is not as sensitive to the presence of chloride or sulphate anions as the chromate anion is. The protective effect of molybdate-based pigments in the presence of chloride or sulphate anions is explained so that the molybdate ions are preferentially adsorbed on the steel surface, giving rise to a complex with ions of iron in the oxidation state +2 (Kalenda *et al.,* 2006; Ruf*,* 1973; Veleva *et al.,* 1999). This coordination compound of iron on its own is unable to form a passivating layer on the steel surface: in fact, only oxidation with oxygen in air gives rise to a coordination compound with iron in the oxidation state +3, which is insoluble and protects the steel surface from corrosion. Hence, the molybdate anion is dependent on the presence of oxygen and is efficient in a weakly basic environment (Farr and Vukasovich, 1986; Kalenda *et al.,* 2006; Ruf*,* 1973). It is unstable in acidic environments, where it decomposes to polymolybdates (Farr and Vukasovich, 1986). Molybdate pigments, such as zinc molybdate, calcium molybdate, and calcium-zinc molybdate, have found application as ingredients in anticorrosion paints intended, for instance, for the protection of ship hulls. In order to benefit from the high anticorrosion efficiency of molybdates while reducing their price, those pigments are manufactured in mixtures with less expensive inorganic fillers or pigments, such as ZnO, lime, or talc (Wicks, 2003). Phosphomolybdates represent the next generation of molybdenum-based anticorrosion pigments. The following phosphomolybdates are frequently used: calcium phosphomolybdate and calcium-zinc phosphomolybdate (Amp *et al.,* 1999).

2. Experimental

2.1 Laboratory preparation of the molybdate-based anticorrosion pigments

Stoichiometric molybdates and core-shell molybdates were prepared in order to use them as pigments in paints intended for the corrosion protection of metals. Molybdates were chosen for detailed examination and the development of pigments owing to their high anticorrosion efficiency (Kalenda *et al.,* 2006). The fact that molybdenum falls into the class of nontoxic elements was considered an important aspect when selecting molybdates as prospective pigments (Bierwagen, 1998). Divalent alkaline earth elements (calcium, strontium, magnesium), zinc, and – from among transition elements – trivalent iron were selected as the cations in the molybdate structure. Strontium, magnesium and calcium are elements forming basic oxides and hydroxides, whereby they may contribute to the inhibition of corrosion.

Preparation of stoichiometric molybdate pigments

Stoichiometric molybdates whose general formula is $Me^{II}(MoO_4)$ or $Me_2^{III}(MoO_4)_3$, where Me = Zn, Ca, Sr, or Mg, were prepared in the laboratory by reactions represented by Equations 1 to 5:

$$1MoO_3 + ZnO \rightarrow ZnMoO_4 \quad (1)$$

$$MoO_3 + CaCO_3 \xrightarrow{-CO_2} CaMoO_4 \quad (2)$$

$MoO_3 + SrCO_3 \xrightarrow{-CO_2} SrMoO_4$ (3)

$MoO_3 + MgCO_3 \xrightarrow{-CO_2} MgMoO_4$ (4)

$2\ Fe_3O_4 + 9\ MoO_3 + ½\ O_2 \rightarrow 3\ Fe_2(MoO_4)_3$ (5)

Preparation of core-shell molybdate pigments

Core-shell molybdate pigments, whose general formulas are $Me^{II}(MoO_4)/CaSiO_3$ and $Me_2^{III}(MoO_4)_3/CaSiO_3$, were prepared by reactions represented by Equations 6 to 10:

$MoO_3 + ZnO + CaSiO_3 \rightarrow ZnMoO_4 / CaSiO_3$ (6)

$MoO_3 + CaCO_3 + CaSiO_3 \xrightarrow{-CO_2} CaMoO_4 / CaSiO_3$ (7)

$MoO_3 + SrCO_3 + CaSiO_3 \xrightarrow{-CO_2} SrMoO_4 / CaSiO_3$ (8)

$MoO_3 + MgCO_3 + CaSiO_3 \xrightarrow{-CO_2} MgMoO_4 / CaSiO_3$ (9)

$2\ Fe_3O_4 + 9\ MoO_3 + ½\ O_2 + CaSiO_3 \rightarrow 3\ Fe_2(MoO_4)_3 / CaSiO_3$ (10)

The synthesis of core-shell molybdates has two assets: the pigment particle shape can be favourably affected, and the amount of incoming molybdenum is reduced. Core-shell molybdates consist of a core, i.e. support, which imparts the shape to the pigment, and a molybdate shell, i.e. a layer coating the core. Natural wollastonite, $CaSiO_3$, was selected as the core. The factors that were taken into account when choosing wollastonite included the needle shape of the primary particles and the basic pH of the aqueous extract, which favourably affects inhibition of the metal corrosion (Kalendová and Veselý, 2009; Sander, 2010). The basicity of the system is also important with respect to the development and stability of the anticorrosion properties of the molybdates (Kalenda *et al.,* 2006). The core-to-shell ($CaSiO_3$-to-molybdate) ratio chosen for the pigments was 9:1.

2.2 Description of the starting materials for the preparation of the pigments

Molybdenum trioxide MoO_3: manufactured by Sigma-Aldrich Chemie, Germany, particle size d_{50} = 20 µm, purity 99%, lemon-yellow colour, melting point 1470°C-1475°C, density 7.16 g/cm^3, M_r 231.838 g/mol.

Ferrous-ferric oxide Fe_3O_4: manufactured by Bayer Chemicals, Germany, magnetite structure, particle size d_{50} = 2 µm, black colour, density 4.7 g/cm^3, M_r 231.533 g/mol.

Calcium carbonate $CaCO_3$: manufactured by Omya GmbH, Austria, calcite structure, particle size d_{50} = 5 µm, density 2.75 g/cm^3, M_r 100.087 g/mol.

Magnesium carbonate $MgCO_3$: imported by Lach-Ner s.r.o., Czech Republic, magnesite structure, density 2.98 g/cm^3, M_r 84.314 g/mol.

Zinc oxide ZnO: manufactured by Slovzink a.s. Košeca, Slovakia, zincite structure, particle size d_{50} = 15 µm, density 2.75 g/cm^3, M_r 81.389 g/mol.

Strontium carbonate $SrCO_3$: manufactured by Sigma-Aldrich Chemie, Germany, strontianite structure, density 3.7 g/cm^3, M_r 147.629 g/mol.

Calcium silicate $CaSiO_3$: imported by Lach-Ner s.r.o., Czech Republic, natural wollastonite (calcium metasilicate) structure, density 2.888 g/cm^3, M_r 319.914 g/mol.

2.3 Procedure for the synthesis of the stoichiometric molybdate pigments and core-shell molybdate pigments

The starting compounds MoO_3, ZnO, $CaCO_3$, $SrCO_3$, $MgCO_3$, Fe_3O_4, and $CaSiO_3$ were weighed with a precision of ±0.01 g in the stoichiometric proportions following Equations 1 to 10. The synthesis procedures for the core-shell molybdates and for the stoichiometric molybdates were identical. The process consisted of the following stages: homogenisation, calcination, and product treatment by rinsing and milling to the required particle size.

The aim of the homogenisation step was not only perfect mixing of the starting materials but also mechanical-chemical activation of the materials, achieving an intimate contact between the particles in the powdered reaction mixture, and increasing the contact area for the reaction. A Dyna-10-therm (Germany) planetary mixing instrument was used for the dry homogenisation. Product homogeneity was improved by conducting the vessel rotation process as a quasi-stochastic process controlled by built-in software (Kaspar and Kuchler, 1998).

For calcination, the homogeneous mixtures of the starting materials were transferred to annealing quartz crucibles, covered with lids because of sublimation of molybdenum, and subjected to the first phase of calcination in an electric furnace. After cooling down, the mixtures were ground in an agate mortar and subjected to the second calcination phase. The calcination temperatures were 750-900°C, depending on the starting substances. The calcined mixtures usually contained residual amounts of the starting substances and/or soluble side products, which may degrade the properties of the pigment. The product was therefore multiply rinsed with distilled water. Since a suitable size of the pigment particles is a very important factor, the calcination step was followed by wet milling, performed in a Pulverisette 6 planetary ball mill (Netzsch, Germany). The powder was placed in a milling container made from zircon-silicate ceramics and milled with rollers made from the same material. The milling time was 60 minutes for the core-shell molybdate pigments and 90 minutes for the stoichiometric molybdate pigments. This step was completed by thorough rinsing of the product. The final product was dried at 110°C for 48 hours.

2.4 Identification of the pigment particle structure and morphology

The X-ray diffraction spectra were measured on an X’pert PRO MPD 1880 X-ray diffractometer (PANanalytical, The Netherlands). The diffraction data were evaluated by means of the X´Pert programs (X´Pert HightScore Plus Software version 2,1b and X´Pert Industry Software version 1.1g); the phases were identified using the ICCD PDF2 diffraction data base. The pigment particle surface and shape were examined on a JEOL-JSM 5600 LV scanning electron microscope (JEOL, Japan) in the secondary electron imaging mode.

2.5 Determination of the physico-chemical properties of the pigment

The pigments' specific weight was determined by using an Autopycnometer 1320 helium pycnometer (Micromeritics, USA). Linseed oil sorption was measured by the pestle-mortar method (Veselý *et al.,* 2010). The outcome, called the oil number (in g/100 g), is a prerequisite for calculation of the CPVC and for the formulation of the paints. The determination of the pH level of aqueous extracts of the pigments was based on the ISO 789-9 standard. Suspensions containing 10% pigments in redistilled water (with a pH of 7 and specific electric conductivity of 3µS/cm) were prepared and the pH was measured with a WTW pH 320 Set-2 multi-processor pH-meter fitted with a glass measuring electrode (WTW Wissenschaftliche Werkstätten, Germany). The pH values were read periodically during a period of 21 days, during which time the pH attained its steady-state level. Ultimately, the suspensions were filtered off and the final pH of the filtrates (extracts) was determined. The filtrates, prepared from 10% aqueous suspensions of the pigments, were then also used to determine the corrosion losses of test metal panels (Kalendová and Veselý, 2009).

Specific electric conductivity data of the aqueous extracts was measured conductometrically. Once again, 10% pigment suspensions in redistilled water were prepared for the measurements. The data were read with a Handylab lF1 conductometer (SCHOTT, Germany), and calibration solutions (37 and 1413 µS/cm at 25°C) were used to obtain correct data. This determination was based on the ISO 787-14 standard. Also again, the readings were made during a period of 21 days, during which time a steady conductivity level was established. The water-soluble fractions of the pigments were determined gravimetrically by a procedure derived from the ČSN EN ISO 787-3 standard (Veselý *et al.,* 2012), i.e. by extraction of the precisely weighed (to ±0.01 g) powdered pigment in distilled water at 20°C (W_{20}) and in boiling water (W_{100}).

2.6 Determination of the corrosion-inhibiting capability of the pigments in the paints

The anticorrosion capability of the pigments as ingredients in paints was evaluated. The efficiency of the paints was assessed based on laboratory tests derived from standardised procedures (Kalendová and Kukačková, 2012).

Formulation and preparation of coating materials containing the pigments tested

Model paints based on a water-based medium-molecular-weight epoxy resin were formulated for investigation of the anticorrosion properties of the pigments. As model formulations, they did not contain any other fillers or additives appreciably affecting the coating material's ultimate efficiency. Pigment volume concentration in the paint was invariably 10 vol.%. Volume concentration of the non-volatile fraction in the paint was adjusted to PVC/CPVC = 0.30 by means of titanium dioxide (TiO_2) as an anticorrosion neutral pigment. The paints were prepared by dispersing in a Dispermat CV pearl mill (WMA Getzmann GmbH, Verfahrenstechnik, Germany). An antifoaming additive and a deflocculating and wetting additive were added to facilitate the dispersing process. The process was conducted at 1200 rpm for 45 minutes. Since the paints were two-component formulations, the procedure of paint application onto the test substrates was preceded by the addition of a hardener to the paint at a hardener-to-resin ratio of 27:100.

Description of the binder

Composition: aqueous dispersion of a 55% solution of the medium-molecular-weight resin, manufactured by Spolchemie a.s., Czech Republic, density 1.03-1.05 g/cm^3, viscosity 0.1 – 0.7 Pa.s, epoxy index 1.88–2.22 mol/kg, non-volatile fraction 55.5%.

Description of the epoxy resin hardener

Composition: aqueous solution of the adduct of the epoxy resin with an amine mixture, manufactured by Spolchemie a.s., Czech Republic, density 1.08 g/cm^3, non-volatile fraction 50%, amine number 130-150 mg KOH/g, viscosity 0.95–1.35 Pa.s at 23°C.

2.7. Test sample preparation

The paint films were applied to the substrates by means of an applicator for steel panels (Q–panel, UK) 152 mm × 102 mm × 0.8 mm size. A total of 10 test panels were prepared for each paint. A thin cut (groove), 10 cm long, which penetrated through the paint film and reached the substrate metal, was made using a sharp blade. Paint films for the adhesion and surface hardness tests were prepared on glass panels with a size of 100 mm × 250 mm. The samples on the test panels were allowed to dry under standard conditions (temperature

20°C, relative humidity 50%) in a conditioned laboratory for 6 weeks. The dry film thickness (DFT) was measured with a Minitest 110 magnetic thickness gauge fitted with a F16 type probe (Elektrophysik, Germany) in accordance with ISO 2808. A 7 mm long test cut was made on the bottom of all steel panels for the corrosion tests.

2.8 Laboratory corrosion tests

In the cyclic corrosion *test with salt mist and condensing moisture*, the test panels were exposed to the mist of a 5% NaCl solution at 35°C ± 2°C for 10 hours (1st cycle stage) and to condensing distilled water at 40°C ± 2°C for 1 hour (2nd cycle stage), followed by drying at 23°C ± 2°C (3rd cycle stage). This test encompassed 25 cycles, i.e. it took 600 hours in total. In the 24-hour cyclic corrosion test in the presence of *condensing water and* SO_2, the test panels were exposed to condensing water containing SO_2 at 36°C ± 2°C for 8 hours (1st cycle stage) followed by drying at 23°C ± 2°C (2nd cycle stage). This test encompassed 15 cycles, i.e. it took 360 hours in total. The third corrosion test was a test with *condensing moisture*, where the panels were exposed to condensing moisture at 38°C ± 2°C for 12 hours (1st cycle stage) followed by drying at 23°C ± 2°C (2nd cycle stage). This test encompassed 15 cycles, i.e. it took 360 hours in total.

Corrosion test evaluation methods

The paint film/substrate metal system evaluation methods following the exposure were based on the ASTM D 714-87, ASTM D 610 and ASTM D 1654-92 standards (Kalendová and Kukačková, 2012). Specifically, the size and frequency of the occurrence of blisters on the paint films were evaluated as per ASTM D 714-87, the fraction of the substrate metal area affected by corrosion was evaluated (after removing the film) as per ASTM D 610, and the distance of propagation of corrosion in the cut (in mm) was evaluated as per ASTM D 1654-92.

Overall evaluation of the anticorrosion efficiency

The changes evaluated based on the ASTM D 1654-92 standard were assigned scores on the Heubach 100-0 scale. Finally, the overall anticorrosion efficiency was calculated based on the three corrosion effects. The overall anticorrosion efficiency encompassing all of the tests (E_{NaCl}, E_{SO2}, and E_{H2O}) was calculated as the arithmetic mean of the scores of the corrosion of the substrate metal, the degree of blister formation, and mean corrosion at the cut (Kalendová and Kukačková, 2012).

Evaluation of the properties of the non-pigmented film

A film of the coating material free from any pigment served as the blank.

2.9 Determination of the pigments' protective efficiency against steel corrosion in aqueous solutions

This corrosion test was performed in an aqueous extract obtained by filtration of a 10% suspension of the powdered pigment tested (Kalendová and Veselý, 2009). Before filtering, the suspensions were allowed to stand for 21 days, during which the constant pH and specific electric conductivity levels were established. This test measured the steel mass loss due to corrosion of the steel sample submerged in the filtrate. Defined steel panels were exposed to the test conditions for 21 days. The values measured were converted to relative corrosion loss data X_{corr} (in %) with respect to the mass loss observed in pure water

(Kalendová and Veselý, 2009).

Reference experiments

A commercial phosphomolybdate-based anticorrosion pigment served as the reference substance. This allowed us to assess the anticorrosion efficiency of the pigments synthesised here. Where the anticorrosion efficiency of paints with our pigments approached that of the paint with the reference pigment, the pigments were regarded as truly anticorrosion efficient. The properties achieved with the pigments were also compared to those achieved with the starting MoO_3. This experiment served as identification of the “background”, in other words, served to ascertain whether the starting substance itself acted as an anticorrosion pigment.

2.10 Physical properties of the paint films

Surface hardness of the paint films

The surface hardness of the films was measured on glass panels with a size of 100 mm × 250 mm, as per ISO 1522, using a pendulum instrument from Persoz (Persoz NF T 30-016 pendulum, Braive Instruments, Belgium). The surface hardness values of the films were converted to relative data (in %) with respect to the hardness of the glass substrate.

Effect of the pigment particles on the paint film adhesion to the substrate

The paint film adhesion to the 100 mm × 250 mm glass panels was evaluated by the cross-cut method, as per ISO 2409. The cut of the lattice pattern was assessed subjectively on the 0-5 scale.

3. Results

3.1 Physico-chemical properties of the powdered pigments

The structure analysis results are given in Table I, and include the crystalline phases identified and the crystal lattice types. The pigment particle morphology is illustrated by scanning electron microscopy photographs for the stoichiometric molybdates in Figure 1 and for the core-shell molybdates in Figure 2. The photographs were taken in the secondary electron imaging (SEI) mode and in the backscattered electron composition (BEC) mode.

The physico-chemical properties of the pigments are given in Table II, including density, linseed consumption, CPVC, pH, specific electric conductivity, and water-soluble fractions W_{100} and W_{20}. The core-shell molybdate and stoichiometric molybdate pigment densities lie within the ranges of 3.01 – 3.07 g/cm^3 and 3.11 – 4.74 g/cm^3, respectively. Oil consumption of the core-shell molybdate pigments lie within the range from 27.41 g/100 g pigment to 33.95 g/100 g pigment, as against the stoichiometric molybdate pigments, where the levels are from 13.88 g/100 g pigment to 31.46 g/100 g pigment. The critical pigment volume concentration levels were calculated to be about from 47% to 52% for the core-shell molybdates and from 49% to 64% for the stoichiometric molybdate pigments. The pH level of the core-shell molybdates lies in the basic region, attaining values from pH 11.0 to pH 12.3, whereas the stoichiometric molybdates are slightly acidic, about pH 4.7 to pH 6.3. The specific electric conductivities of the core-shell molybdates were 270 µS/cm for $Fe_2(MoO_6)_3/CaSiO_3$, 1840 µS/cm for $MgMoO_4/CaSiO_3$, 890 µS/cm for $ZnMoO_4/CaSiO_3$, and 6620-6960 µS/cm for $SrMoO_4/CaSiO_3$ and $CarMoO_4/CaSiO_3$. The cold water-soluble (W_{20}) fraction exhibited values from 0.55% to 1.92% (depending on the cation) for the core-shell molybdate pigments and from 0.40% to 1.64% for the stoichiometric molybdate pigments.

The hot water-soluble fraction (W_{100}) exhibited values from 0.58% to 3.04% for the core-shell molybdate pigments and from 0.76% to 1.79% for the stoichiometric molybdate pigments.

Take in Table I

Take in Figure 1

Take in Figure 2

Take in Table II

3.2 Steel corrosion losses in the aqueous extracts of the pigments

The relative steel corrosion losses (X_{corr}) are given in Table III along with the pH and specific electric conductivity (χ) data measured on the 1st (pH_1, χ_1) and 21st (pH_{21}, χ_{21}) days of the test. The specific electric conductivities (χ_1) of the core-shell molybdates ($CaMoO_4/CaSiO_3$ and $SrMoO_4/CaSiO_3$) lay within the region of 6.25 $.10^3$ to 6.23,10^3 µS/cm, as against the stoichiometric pigments, where they were as low as 687 to 326 µS/cm. The specific electric conductivities of the core-shell molybdates ($MgMoO_4/CaSiO_3$ and $ZnMoO_4/CaSiO_3$) lay within the region of 1.70 $.10^3$ to 0.79.10^3 µS/cm, as against the stoichiometric pigments, where they 2.7.10^3 to 2.0.10^3 µS/cm. The pH_1 was from pH 11.5 to ph 12.4 for the core-shell pigments, and it was lower, from pH 5.2 to pH 6.4, for the stoichiometric pigments. The corrosion weight loss levels in the aqueous extracts of the paint films were from 43% to 79% for the core-shell molybdates and from 44% to 72% for the stoichiometric molybdates.

Take in Table III

3.3 Corrosion tests

The results of the corrosion test of the paints with the pigments in the environment of *condensed water containing SO_2* are given in Table IV. The size and frequency of blisters in the paint film were determined as per ASTM D 714-87, the fraction of substrate metal area affected by corrosion was determined as per ASTM D 610, the distance of propagation of corrosion in the cut was determined after removing the paint film as per ASTM D 1654-92, and the overall anticorrosion efficiency (E_{SO2}) was calculated as described above. The results of the corrosion test of the paints with the pigments in the environment of *condensed water* and the calculated overall anticorrosion efficiency E_{H2O} are given in Table V. The results of the corrosion test of the paints with the pigments in the environment of *NaCl mist* and the calculated overall anticorrosion efficiency E_{NaCl} are given in Table VI.

Corrosion on the metal surface in the atmosphere with SO_2 beneath the film, was from <0.01% to 0.1 % for core-shell molybdates. Corrosion on the metal surface, was from <0.01% to 33 % for stoichometric molybdates. Metal corrosion in the cut was 2-3 mm or >16 mm for the two molybdate pigment types. Film blistering on the paint film in the atmosphere with NaCl was few and medium degree for stoichiometric molybdate pigments. No blisters on the film surface were found for any of the core-shell molybdate pigments except $CaMoO_4$ /$CaSiO_3$ (6F). The levels of blistering in the environment with condensing water were different for the core-shell molybdates. Film blistering was very low for the stoichiometric molybdates. Metal surface corrosion beneath the film was very low, viz. from <0.3% to 3% for the core-shell pigments and from <0.01% to 33 % for the stoichiometric pigments.

Take in Table IV

Take in Table V

Take in Table VI

3.4 Effect of the pigments on the physical properties of the paint films

The data of surface hardness and adhesion of the paint films with the pigments are given in Table VII.

Take in Table VII

4. Discussion

4.1 Structure and morphology of the pigments

The structure of the stoichiometric molybdates and core-shell molybdates was elucidated by X-ray diffraction analysis. The stoichiometric molybdate-based pigments exhibited a high degree of structural purity, free from traces of the starting substances. The core-shell pigments contained calcium consisted of wollastonite as the core and powellite ($CaMoO_4$) as the shell. Other metal ions – Sr, Zn, Mg, and Fe –isomorphically substituted the Ca ions in the crystal lattice. SEM photographs showing the morphology of the particles are reproduced in Figures 1 and 2. The core-shell molybdate particles possess a non-isometric shape due to the wollastonite core, whereas the stoichiometric molybdate particles exhibit a highly regular, isometric shape.

4.2 Physico-chemical properties of the powdered pigments

The water-soluble fraction

The specific weights of the stoichiometric molybdates lay within the range of 3.1-4.7 g/cm^3 depending on the divalent or trivalent cation content (Table II). The specific weights of the core-shell molybdates lay within the range of 3.1-3.7 g/cm^3. The specific weights of the matching counterparts of the core-shell molybdates decreased due to the effect of the core. The linseed consumption data depended on the particle size and shape, specific surface area, and porosity. Due to the presence of wollastonite, the CPVC values were lower for the core-shell molybdates than for the stoichiometric molybdates.

The soluble fraction was determined in distilled boiling water (100°C) and at 23°C. The data provide information on substances that are extractable into water or that dissociate in water. A water-soluble fraction that is too high adversely affects both the stability of the pigmented binder and the liquid coating material during storage, as well as the properties of the cross-linked paint films. Soluble substances affect the stability of the dispersion systems, i.e. the liquid coating material containing the pigments. They also affect the osmotic processes in the pigmented polymeric film. Identification of a generally applicable “critical” water-soluble fraction is impossible because it is affected by the type of binder, pigment concentration, and total formulation of the paint. However, a certain amount of water-soluble substances is desirable to make the pigment active in chemical reactions during the corrosion processes. From the stoichiometric molybdates, the highest water-soluble fractions were found for the pigments $MgMoO_4$ (W_{100}=1.79%) and $CaMoO_4$ (W_{100}=1.00%), which are pigments that quite readily release the bulky Mg^{2+} and Ca^{2+} cations from the crystal lattice. The stoichiometric molybdate $Fe_2(MoO_4)_3$ exhibited a relatively low fraction soluble in water at room temperature (W_{20} = 0.532%). Whether this level is also optimal with respect to the corrosion protection capability of the paint film containing this pigment will be apparent from the corrosion tests, particularly in the environment with condensed moisture. The formation of osmotic blisters is a manifestation of too high a water-soluble fraction, which passes from the pigment to the polymeric film.

From among the core-shell molybdates, the lowest fraction of substances that are soluble in hot water, W_{100} = 0.582%, was found in the pigment containing the Fe^3 cations, i.e. $Fe_2(MoO_4)_3/CaSiO_3$, whereas the highest fractions were found in the pigments $SrMoO_4/CaSiO_3$ (W_{100} = 3.04%) and $CaMoO_4/CaSiO_3$ (W_{100} = 2.72%).

Summary information gained from the data on the water soluble fractions is as follows:

- The core-shell molybdates contain a higher water-soluble fraction than the stoichiometric molybdates.
- The fraction of substances that are soluble in hot water is higher than the fraction of substances that are soluble in water at room temperature.
- Pigments containing the divalent Mg and Ca cations possessed a higher water-soluble fraction than those containing the trivalent Fe cations. The Ca, Sr, and Mg cations are rather readily released from the crystal lattice and the pigments are more soluble.
- The lowest fractions of substances soluble in hot water (W_{100}) were found in stoichiometric molybdates containing the Fe^{3+} cations.

Acid-base properties of the pigments

The amount of acid or basic components in a pigment is an important parameter, suggesting a potential effect on the corrosion reactions at the metal-paint film interface. This parameter affects the acid-base properties of the pigmented paint film when in contact with an aqueous environment. This is a property of the pigments that also subsequently affects the chemical resistance of the paint films containing them. Too high alkalinity (high pH) of the pigment may result in the degradation of bonds of the binder, which contains functional groups that are prone to saponification. Too high acidity (low pH) of the pigment also induces reactions that adversely affect the stability of the binder and lifetime of the paint film in a manner similar to the effect of too high alkalinity. Within 21 days, the pH of aqueous extracts of the stoichiometric molybdates and core-shell molybdates attained constant levels within the ranges of 4.0-6.3 and 10.5-12.3, respectively (Table II).

Summary information gained from the pH measurements is as follows:

- The pH of the core-shell molybdate-based pigments was shifted to the basic region due to the presence of wollastonite, whose aqueous extract exhibits pH 9.9. The highest pH levels measured over 21 days were found for $CaMoO_4/CaSiO_3$ (pH = 12.3) and $SrMoO_4/CaSiO_3$ (pH = 12.1). Core-shell molybdate-based pigments with iron, i.e. $Fe_2(MoO_4)_3/CaSiO_3$, exhibited lower pH levels (pH =11.0).
- Stoichiometric molybdates with Fe exhibit pH values which are more shifted to the acid or weakly basic region than with the stoichiometric molybdates with Ca, Sr, Mg, whose pH lies in the basic region, similarly to core-shell molybdates.

Specific electric conductivity of aqueous extracts of the pigments

The specific electric conductivity of all aqueous extracts of the pigments increased with time; this indicates a slow release of ions from the pigments' crystal lattice. To an extent, there is an analogy between specific conductivity and the water-soluble fraction. An optimum specific electric conductivity of the aqueous solutions diffusing through the film is important in corrosion reactions suppressing or slowing down partial anodic or cathodic reactions. The specific electric conductivity levels of the aqueous extracts of the stoichiometric molybdate-based pigments measured over 21 days occupied the region of 176-2810 µS/cm, depending on the pigment's chemical composition. The lowest value – 176 µS/cm – was found for $Fe_2(MoO_4)_3$. For the core-shell pigments, the specific electric conductivity region at 21 days was 270-6960 µS/cm, again depending on the pigment's chemical composition. The lowest value – 270 µS/cm – was found for $Fe_2(MoO_4)_3/CaSiO_3$.

Summary information gained from the specific electric conductivity measurements is as follows:

- The core-shell molybdates exhibit higher specific electric conductivity levels than the stoichiometric molybdates.
- A direct proportionality correlation exists between the activity levels of the core-shell molybdates containing Ca, Mg, or Sr and the water-soluble fractions.

4.3 Corrosion losses of the steel panels in the aqueous extracts of the pigments

Corrosion losses characterise the metal's resistance to corrosion in the aqueous extract of the pigment, in which ions passivating the metal surface are present. Data on corrosion losses of metals in the extracts provide guidance regarding the suitability of the pigment as an ingredient for anticorrosion coating materials. The corrosion loss should be highest in pure water, where no ions released from the pigment and passivating the surface of the metal are present. Thus, the relative corrosion loss calculated with respect to the corrosion loss in distilled water (Kalendová *et al.,* 2008) is an illustrative criterion for assessing the pigments' corrosion-inhibiting capability. The pH and specific electric conductivity levels in the filtrates with steel panels submerged in them were measured periodically during the test. In nearly all of the extracts, corrosion was accompanied by a decrease in the specific conductivity, due to the precipitation of ions on the metal surface and, hence, a decrease in their concentration in the solution. Summary information gained from the corrosion loss measurements is as follows (Table III):

- Extracts from the core-shell molybdates exhibited a somewhat higher level of protection of the metal surface than extracts from the stoichiometric molybdates. This was due to their pH, which lay in a region where steel does not corrode appreciably. Specific conductivity, where the results are not that unambiguous, is a less important factor. The Mo content does not play a major role when considering the fact that the Mo content of the core-shell molybdates is roughly one-tenth that of the stoichiometric molybdates.
- In the class of core-shell molybdates, the lowest corrosion losses were found in the extracts of $FeMoO_4/CaSiO_3$ (42.53%), $SrMoO_4/CaSiO_3$ (45.14%), and $MgMoO_4/CaSiO_3$ (46.85%).
- In the class of stoichiometric molybdates, the lowest corrosion loss was found in the extract of $SrMoO_4$ (43.93%).
- Corrosion losses in the extracts of the majority of the molybdate pigments were lower than in the extract of the reference pigment.

4.4 Corrosion-inhibiting properties of the pigments in the paints

4.4.1 Corrosion test in the atmosphere with SO_2

Paint films in the condensation chamber were exposed to the atmosphere with SO_2 for 360 hours (Table IV). In the class of stoichiometric molybdates, the highest anticorrosion efficiency was found with $Fe_2(MoO_4)_3$, where the overall anticorrosion efficiency score was 87. The score of the film containing the reference pigment was somewhat lower (82). In the class of core-shell molybdates, the overall anticorrosion efficiency scores lay within the range of 60-87, with the highest score (87) being found for the paint film with $Fe_2(MoO_4)_3/CaSiO_3$.

The overall anticorrosion efficiency of core-shell and stoichiometric pigments did not differ appreciably; the core-shell molybdates exhibited a very slightly lower anticorrosion efficiency than the stoichiometric molybdates. Paint films pigmented with core-shell molybdates exhibited better results in substrate corrosion protection as compared to stoichiometric molybdates. This suggests that, owing to the favourable shape of the primary particles, it is more difficult for SO_2 to diffuse through the film. Core-shell molybdates also contain, in addition to molybdate, $CaSiO_3$, whose particle shape contributes favourably to the paint's anticorrosion efficiency (Kalenda *et al.,* 2006). Actually, the MoO_3 content of the core-shell pigment $Fe_2(MoO_4)_3/CaSiO_3$ is roughly one-tenth that of the stoichiometric $Fe_2(MoO_4)_3$. The high pH level of the core-shell pigments is also beneficial to the metal surface passivating effect.

Summary information gained from the pigment exposure to the atmosphere with SO_2 is as follows:

- As regards the overall anticorrosion efficiency of the pigments synthesised in comparison to the reference pigment, the efficiency of the stoichiometric molybdates decreases in the order: $Fe_2(MoO_4)_3$ (87), reference anticorrosion pigment (82), $ZnMoO_4$ (72).
- The efficiency of core-shell molybdates decreases in the order: $Fe_2(MoO_4)_3/CaSiO_3$(87), reference anticorrosion pigment (82), $SrMoO_4/CaSiO_3$ (78), $SrMoO_4/CaSiO_3$ (77).
- All paints with the pigments exhibited a higher efficiency than the non-pigmented coating materials.
- Both stoichiometric molybdates and core-shell molybdates containing Ca exhibited a lower anticorrosion efficiency.
- Anticorrosion efficiencies better than that of the paint with the reference pigment were found for paints with the pigments $Fe_2(MoO_4)_3/CaSiO_3$ and $Fe_2(MoO_4)_3$.

Selected photographs of the test panels following exposure to the environment with SO_2 are shown in Figure 3.

Take in Figure 3

4.4.2 Corrosion test in the atmosphere with condensing water

The highest anticorrosion efficiency was achieved with paints pigmented with the stoichiometric molybdates $Fe_2(MoO_4)_3$ (98), $CaMoO_4$ (98), and $MgMoO_4$ (98). Among the core-shell molybdates, the highest overall anticorrosion efficiency score (70) was achieved with paints pigmented with $Fe_2(MoO_4)_3/CaSiO_3$ (Table V). The failure of the core-shell molybdates as compared to the stoichiometric molybdates can be explained in terms of their higher solubility, which affects their behaviour in the chamber with condensing water at an elevated temperature. The total time of exposure to the condensed moisture or degree of wetting was longest in this test (12 hours at 40°C). The most frequent reason for the failure of anticorrosion properties was a higher water-soluble fraction, which is responsible for the more extensive formation of blisters. The lowest overall anticorrosion efficiency was observed with the coating containing no pigment. The polymeric cross-linked film, with no major pores or inhomogeneities, as is the case with pigmented films, formed a barrier between the metallic surface and the environment with adhesion-physical properties, which were limited by the properties of the binder. Since no ideally impermeable and nonporous binder exists, the precondition for the occurrence of electrochemical corrosion, i.e. the presence of water on the metal surface, is always met. Where no pigment with corrosion-inhibiting properties was present, corrosion developed independent of factors such as the binder type and drying mechanism, film thickness, number of coats, and metal surface treatment procedure prior to applying the coating (Perera, 2004). A comparison of results observed with the films with and without an anticorrosion pigment provided insight into the pigment's contribution to the chemical and corrosion resistance of the binder.

Summary information gained from the pigment exposure to an atmosphere with condensed moisture is as follows:

- Higher overall anticorrosion efficiency levels were observed with the stoichiometric molybdates, which exhibited better protection against corrosion in the cut and a lower tendency to form blisters in the film. Core-shell molybdates exhibited lower anticorrosion efficiency levels than stoichiometric molybdates. This can be explained in terms of a higher water-soluble fraction, which is a critical factor in this atmosphere.
- As regards the overall anticorrosion efficiency of the pigments synthesised in comparison to the reference pigment, the efficiency of the stoichiometric molybdates decreases in the order: $Fe_2(MoO_4)_3$(98), $CaMoO_4$ (98), $MgMoO_4$ (98), $ZnMoO_4$ (90), reference anticorrosion pigment (55), $SrMoO_{4,}$ (50).
- The overall anticorrosion efficiency of core-shell molybdate-based pigments decreases in the order: $Fe_2(MoO_4)_3/CaSiO_3$ (70), $MgMoO_4.Fe_2(MoO_4)_3/CaSiO_3$ (67), $CaMoO_4/CaSiO_3$ (63), reference pigment (55).
- Both the stoichiometric molybdates and core-shell molybdates containing Sr exhibit a lower anticorrosion efficiency.
- The majority of the pigments prepared exhibited a higher efficiency in the paints than the reference anticorrosion pigment.

Photographs of the panels following exposure to the atmosphere with condensed moisture are shown in Figure 4.

Take in Figure 4

4.4.3 Corrosion test in the atmosphere with neutral salt mist

The overall anticorrosion efficiency values E_{NaCl} of paint films pigmented with stoichiometric molybdates occupied a region up to the score 80, with the highest value being found for the paint with $Fe_2(MoO_4)_3$. In the core-shell molybdate class, the overall anticorrosion efficiency of the pigmented paints was found to lie within the range of 58-83, with the highest levels being found for the paints containing $MgMoO_4/CaSiO_3$ (83) and $ZnMoO_4/CaSiO_3$ (80). The higher alkalinity of core-shell molybdates as compared to stoichiometric molybdates and the shape of the primary particles created a better barrier to the penetration of NaCl into the paint film (Table VI). The alkaline extract of the pigment enhanced the corrosion protection of the substrate metal. The excess $CaSiO_3$ that was present in the pigments also contributed to the protection against diffusion of the chloride ions. The least efficient coating materials included the paint pigmented with MoO_3 and the coating material without any pigment. The extract of MoO_3 alone was rather acid; therefore, this substance on its own is unable to adsorb on the metal surface and passivate it. The overall anticorrosion efficiency score of the reference anticorrosion pigment was 58.

Summary information gained from the pigment exposure to an atmosphere with NaCl mist is as follows (Table VI):

- The efficiency of stoichiometric molybdate-based pigments decreases in the order: $Fe_2(MoO_4)_3$ (80), $Zn(MoO_4)_3$ (73)
- The efficiency of core-shell molybdate-based pigments decreases in the order: $MgMoO_4$/ $CasiO_3$ (83), $ZnMoO_4/CaSiO_3$ (80), $Fe_2(MoO_4)_3/CaSiO_3$ (78), $SrMoO_4/CaSiO_3$ (78)
- The core-shell molybdates exhibited somewhat better overall anticorrosion efficiency than the stoichiometric molybdates.
- Core-shell molybdates were more efficient against diffusion of Cl^- ions, neutralising them and forming a physical barrier by reinforcing the paint film. Paints with molybdates containing Fe were the most active against the action of the NaCl mist.
- Both stoichiometric molybdates and core-shell molybdates containing Ca exhibited a lower anticorrosion efficiency, specifically a low ability to prevent corrosion in the cut and formation of blisters.

Photographs of the panels following exposure to the atmosphere with NaCl mist are shown in Figure 5.

Take in Figure 5

4.5 Effect of the pigments on the physical properties of the paint films

The paint films containing the pigments tested exhibited outstanding adhesion (see Table VII); the degree of adhesion was 0 and 1 for all of them. Paint films containing the stoichiometric molybdate-based pigments possessed lower surface hardness levels; the surface hardness of the paint film with $SrMoO_4$ approached that of the non-pigmented coating material (61.6%). Higher surface hardness levels (54.1%-63.5%) were attained with paint films containing core-shell molybdate-based pigments. This fact can be ascribed to the high hardness of wollastonite, which is a silicate mineral. Core-shell molybdate-based pigments have a favourable effect on the hardness and the drying process of the paint films.

5. Conclusions

When comparing the anticorrosion efficiency of paint films pigmented with stoichiometric molybdates and with core-shell molybdates, somewhat higher levels were found for the former class, i.e. paint films pigmented with stoichiometric molybdates exhibited slightly higher anticorrosion efficiency than paint films with core-shell molybdate pigments.

The highest corrosion-inhibiting ability in the environment with SO_2 was found for $Fe_2(MoO_4)_3$ among the stoichiometric molybdates and for $Fe_2(MoO_4)_3/CaSiO_3$ among the core-shell molybdates.

A high corrosion-inhibiting efficiency against the action of chloride ions in the environment with salt mist was found for the stoichiometric molybdate $Fe_2(MoO_4)_3$ and for the core-shell molybdates $Fe_2(MoO_4)_3/CaSiO_3$, $MgMoO_4/CaSiO_3$ and $ZnMoO_4/CaSiO_3$. A high corrosion-inhibiting efficiency against condensed moisture was observed with the stoichiometric molybdate containing ferric cations, $Fe_2(MoO_4)_3$. Among core-shell molybdates, $MgMoO_4/ CaSiO_3$ exhibited a high corrosion-inhibiting efficiency. Overall, pigments containing ferric ions, specifically $Fe_2(MoO_4)_3$, provided the best results among pigments of either class. Paint films containing those pigments exhibited the best results in all of the accelerated corrosion tests, even better than those attained with the reference anticorrosion pigment.

The pigments tested all had a favourable effect on the physical properties of the coating material binder.

Finding from the corrosion tests can be summarised as follows:

1. When the paint films are exposed to corrosion environments with SO_2 or with condensed moisture, it is the Mo content rather than the wollastonite content that governs the pigment's anticorrosion efficiency, whereas the wollastonite content is more important when the paint films are exposed to the NaCl mist.
2. Stoichiometric molybdates containing Fe, Zn and Mg emerge as pigments whose overall anticorrosion efficiency is higher than that of the reference pigment. Among stoichiometric molybdates, the presence of the Fe cation is more important for the corrosion-inhibiting efficiency of the pigment. The Ca and Sr cations cause deterioration of the properties of the stoichiometric molybdates in that the occurrence of blisters is higher with these cations. With respect to the anticorrosion efficiency of the paint, the suitability of cations for the molybdate structure decreases in the order: Fe>>Zn>Mg>Ca.
3. Core-shell molybdates containing Fe, Mg, or Sr also emerged as pigments whose overall anticorrosion efficiency is higher than that of the reference pigment. With respect to the anticorrosion efficiency of the paint, the suitability of cations for the molybdate structure decreases in the order: Fe>Mg >Sr≈Zn>Ca.
4. The mechanism of action of the pigments can be seen in the electrochemical pH shift to a range where steel is in its passive state and hence, does not corrode. The chemical mechanism consists of the formation of protective layers at the metal-pigment interface. This is documented by the decrease in conductivity while the panels corrode. The barrier mechanism, present owing to the wollastonite content, contributes to the pigments' efficiency.

References

Amo, B., Romagnoli, R., Deyá, C. and González, J.A. (2002), *“High performance water-based paints with non-toxic anticorrosive pigments”*, Progress in Organic Coatings, Vol. 45, pp. 389–397.

Amo, B., Romagnoli, R. and Vetere, V.F. (1999), *“Performance of zinc molybdenum phosphate in anticorrosive paints by accelerated and electrochemical tests”*, Journal of Applied Electrochemistry, Vol. 29, pp. 1401-1407.

Bethencourt, M., Botana F.J., Marcos, M., Osuna, R.M. and Sánchez-Amaya, J.M. (2003) *“Inhibitor properties of “green”pigments for paints”*, Progress in Organic Coatings, Vol. 46, pp. 280–287.

Bierwagen G.P. (1998), Organic Coatings for Corrosion Control, ACS Symposium Series 698, Oxford University press, Oxfords, United States of America, pp. 356-365.

Blustein, G., Deyá, M.C., Romagnoli, R. And Amo, B. (2005), *“Three generations of inorganic phosphates in solvent and water-borne paints: A synergism case”*, Applied Surface Science, Vol. 252, pp. 1386–1397.

Deyá, M.C., Blustein, G., Romagnoli, R. and Amo, B. (2002), *“The influence of the anion type on the anticorrosive behaviour of inorganic phosphates”*, Surface and Coatings Technology, Vol. 150, pp. 133–142.

Kalenda, P., Kalendová, A. and Veselý, D. (2006), *“Properties of anticorrosion pigments depending on their chemical composition and PVC value”,* Pigment & Resin Technology, Vol. 35, pp. 188-199.

Kalendová, A. and Veselý, D. (2009),*“Study of the anticorrosive efficiency of zincite and periclase-based core- shell pigments in organic coatings”,* Progress in Organic Coatings, Vol. 64, pp. 5–19.

Kalendová, A., Veselý, D. and Stejskal, J. (2008), *“Organic coatings containing polyaniline and inorganic pigments as corrosion inhibitors”*, Progress in Organic Coatings, Vol. 62, pp. 105–116.

Kuchler, M. and Kaspar, T. (1998), *“Das Vermenget der Rohstoffe zir Pigmentenherstellung in einem Mischer mit Stochastischer Behalterbewegung”*, Scientific papers of the University of Pardubice, Series A, Faculty of Chemical technology. Vol. 4, pp. 151-159.

Kukačková, H. and Kalendová, A. (2012), *“Investigation of mechanical resistance and corrosion-inhibition properties of surface-modified fillers with polyaniline in organic coatings”*, Journal of Physics and Chemistry of Solids, Vol. 73, pp. 1556–1561.

Mahdavian, M. and Attar, M.M. (2005), *“Evaluation of zinc phosphate and zinc chromate effectiveness via AC and DC methods“*, Progress in Organic Coating, Vol. 53, pp. 191–194.

Naderi, R. and Attar, M.M. (2009), *“The inhibitive performance of polyphosphate – based anticorrosion pigments using electrochemical techniques”,* Dyes Pigments, Vol. 80, pp. 349–354.

Naderi, R. and Attar, M.M. (2008), *“Electrochemical assessing corrosion inhibiting effects of zinc aluminium polyphosphate (ZAPP) as a modified zinc phosphate pigment”*, Electrochemica Acta, Vol. 53, pp. 5692–5696.

Naderi, R. and Attar, M.M. (2009), *“The inhibitive performance of polyphosphate – based anticorrosion pigments using electrochemical techniques”*, Dyes Pigments, Vol. 80, pp. 349–354.

Naderi, R. and Attar, M.M. (2009), *“Electrochemical study of protective behaviour of organic coating pigmented with zinc aluminium polyphosphate as a modified zinc phosphate at different pigment“*, Progress in Organic Coating, Vol. 66, pp. 314–320.

Perera, D.Y. (2004), *”Effect of pigmentation on organic coating characteristics”,* Progress in Organic Coatings, Vol. 50, pp. 247–262.

Ruf, J. (1973), *“Unbunte Korrosionsschutz pigmente“*, Farbe und Lack, Vol. 19, pp. 22-27.

Sander, J. (2010), *“Anticorrosive coatings: Fundamentals and New concepts”*, Hanover: Vincentz Network, pp. 215.

Veleva, L., Chin, J. and Amo, B. (1999), *“Corrosion electrochemical behaviour of epoxy anticorrosive paints based on zinc molybdenum phosphate and zinc oxide”*, Progress in Organic Coatings, Vol. 36, pp. 211–216.

Veselý, D., Kalendová, A. and Kalenda, P. (2010), *"A study of diatomite and calcined kaoline properties in anticorrosion protective coatings",* Progress in Organic Coatings, Vol. 68, pp. 173–179.

Veselý, D. ,Kalendová, A. and Manso, M.V. (2012), *"Properties of calcined kaolins in anticorrosion paints depending on PVC, chemical composition and shape of particles"*, Progress in Organic Coatings, Vol. 74, pp. 82–91.

Vukasovich, M.S. and Farr, J.P.G. (1986), *"Molybdate in corrosion inhibition – a review",* Polyhedron, Vol. 5, pp. 551–559.

Wicks, Z. W. (2003), Organic coatings for corrosion control, Kirk-Othmer Encyclopedia of Chemical Technology, pp. 167 – 189.

Zubielewicz, M. and Gnot, W. (2004), *"Mechanisms of non-toxic anticorrosive pigments in organic waterborne coatings"*, Progress in Organic Coatings, Vol. 49, pp. 358–371.

Corresponding author
T.Hájková can be contacted at*:* hajkova.ttereza@seznam.cz

About the authors

Kalendová A. is currently a Professor and a guarantor of the research laboratory for pigments and fillers operating in the framework of the Institute of Chemistry and Technology of Macromolecular Materials at the University of Pardubice. Andréa Kalendová was graduated in the field of Analytical Chemistry with orientation to the environment protection in 1987 and gained her PhD at the Institute of Chemical Technology of the University of Pardubice in 1996. She devotes her efforts to the research and development of advanced nontoxic anticorrosive pigments. Besides the syntheses alone there are studied also mechanisms of anticorrosion actions of appropriate pigments in the coatings. Further she is engaged in the development of corrosion methods for evaluation of the organic coatings. Her experimental work resulted in 70 publications, overwhelmingly in chemical technology journals.

Hájková T. was graduated at the Institute of Chemical Technology at Pardubice in 2013. She finished the Master's degree in Chemistry at the Institute of Chemistry and Technology of Macromolecular Materials in 2013 with the diploma thesis on the the Anticorrosion and physical properties of polymeric alkyd films depending on the pigment structure and filler content. The main regions of her interest as a specialist are non toxic pigments (perovskites, metal oxide pigments) the synthesis thereof, the properties in connection to organic coatings. This topic is also the subject of his PhD which he started on October 2013. Her experimental work resulted in 2 publications in chemical technology journals.

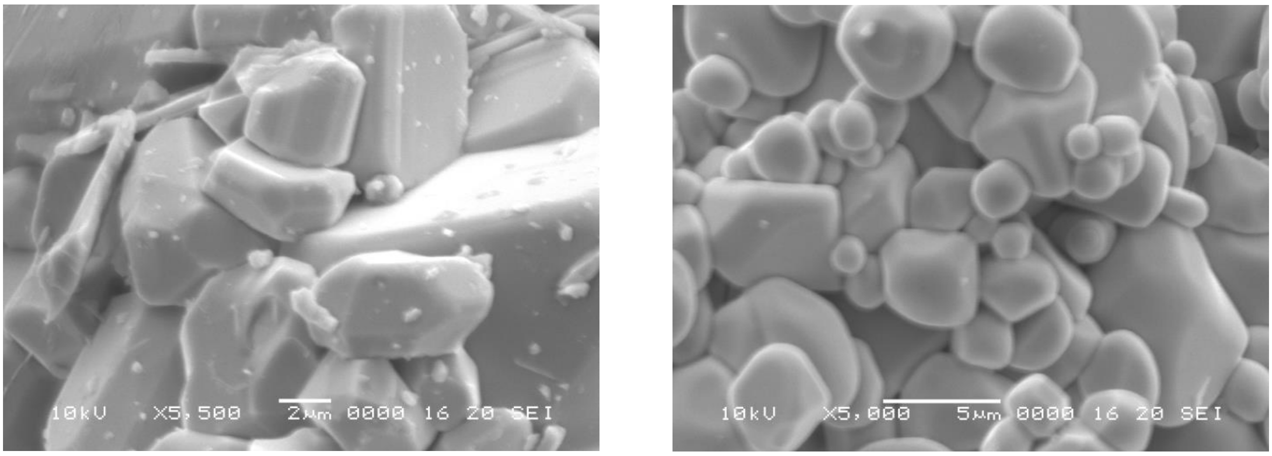

(a) Magnification 5500×, SEI mode (b) Magnification 5000×, SEI mode

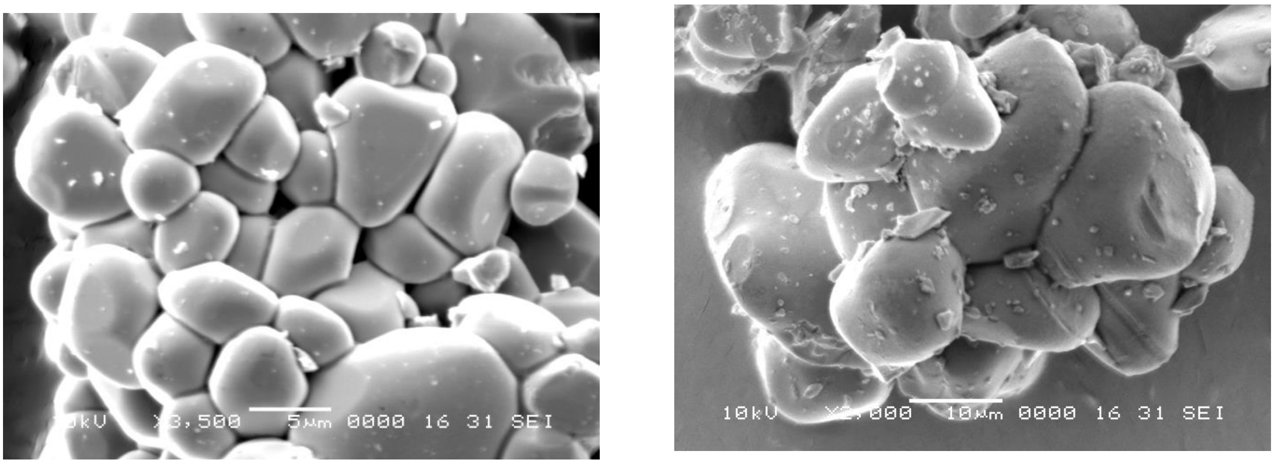

(c) Magnification 3500×, SEI mode (d) Magnification 2000×, SEI mode

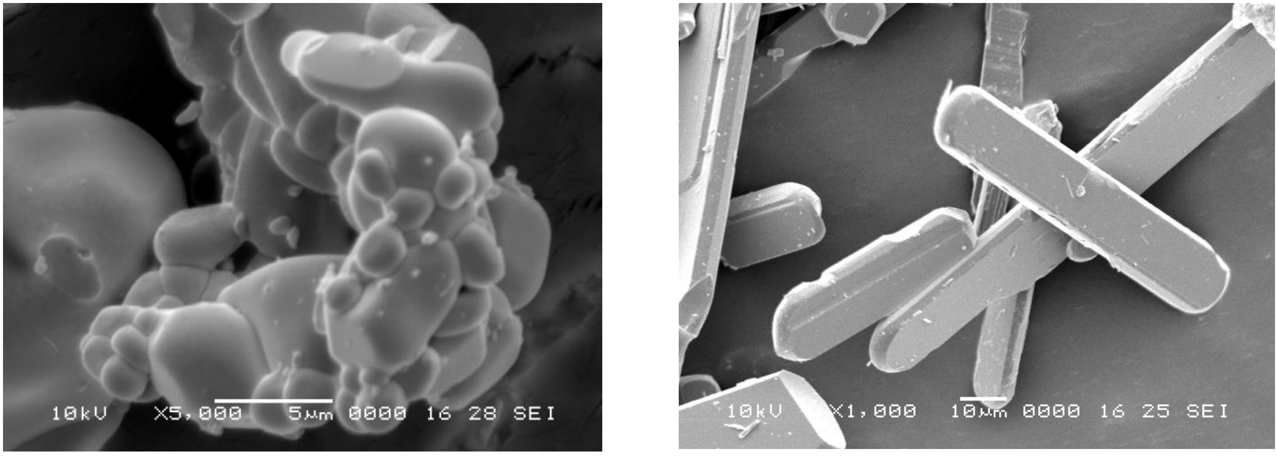

(e) Magnification 5000×, SEI mode (f) Magnification 1000×, SEI mode

Figure 1 SEM photographs of the stoichiometric molybdate particles, SEI detector:

a) $ZnMoO_4$; b) $CaMoO_4$; c) $SrMoO_4$; d) $MgMoO_4$; e) $Fe_2(MoO_4)_3$, f) MoO_3.

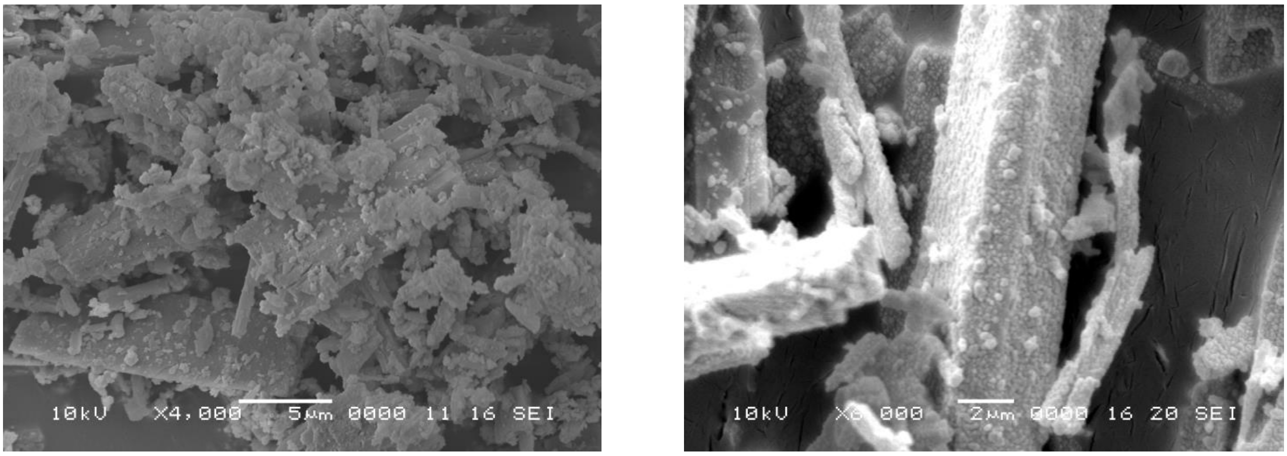

(a) Magnification 4000×, SEI mode (b) Magnification 6000×, SEI mode

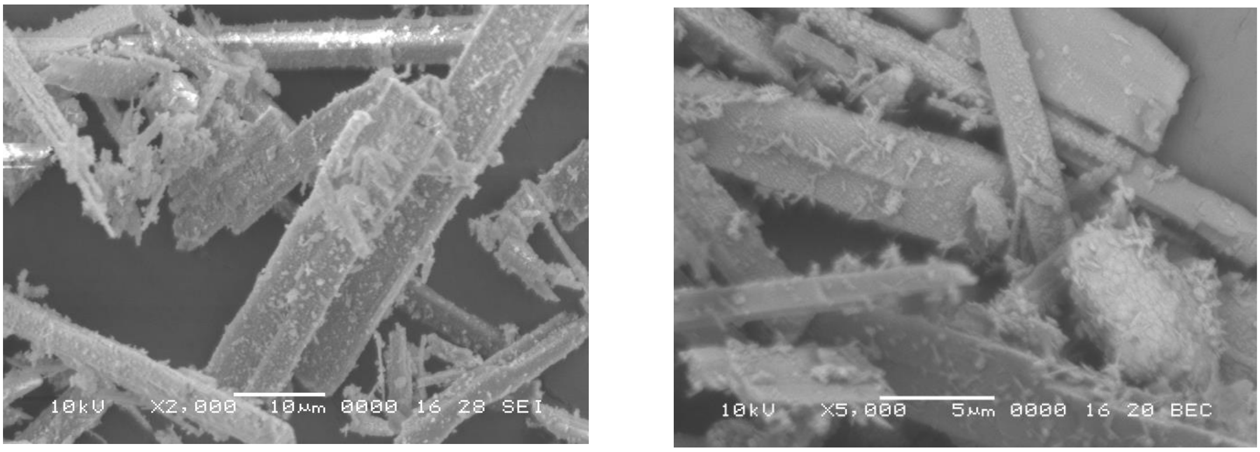

(c) Magnification 2000×, SEI mode (d) Magnification **5**000×, BEC mode

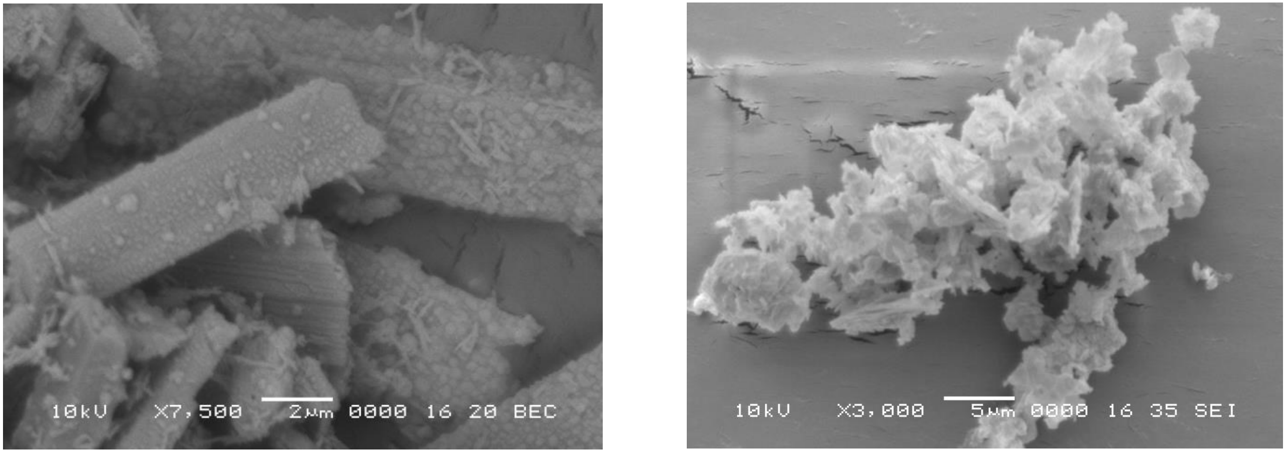

e) Magnification 7500×, BEC mode (f) Magnification 3000×, SEI mode

Figure 2 SEM photographs of the core-shell molybdate particles: a) $ZnMoO_4/CaSiO_3$; b) $CaMo_4/CaSiO_3$; c) $SrMoO_4/CaSiO_3$; d) $MgMoO_4/CaSiO_3$; e) $Fe_2(MoO_4)_3/CaSiO_3$; (f) reference pigment

$Fe_2(MoO_4)_3$ Non-pigmented film $Fe_2(MoO_4)_3$ /$CaSiO_3$.

Figure 3 Results of the corrosion tests of panels coated with the paint films and exposed to SO_2. Paints with $Fe_2(MoO_4)_3$. The top of each photograph shows the paint film surface with the cut, the bottom shows the metal surface after removing the coating.

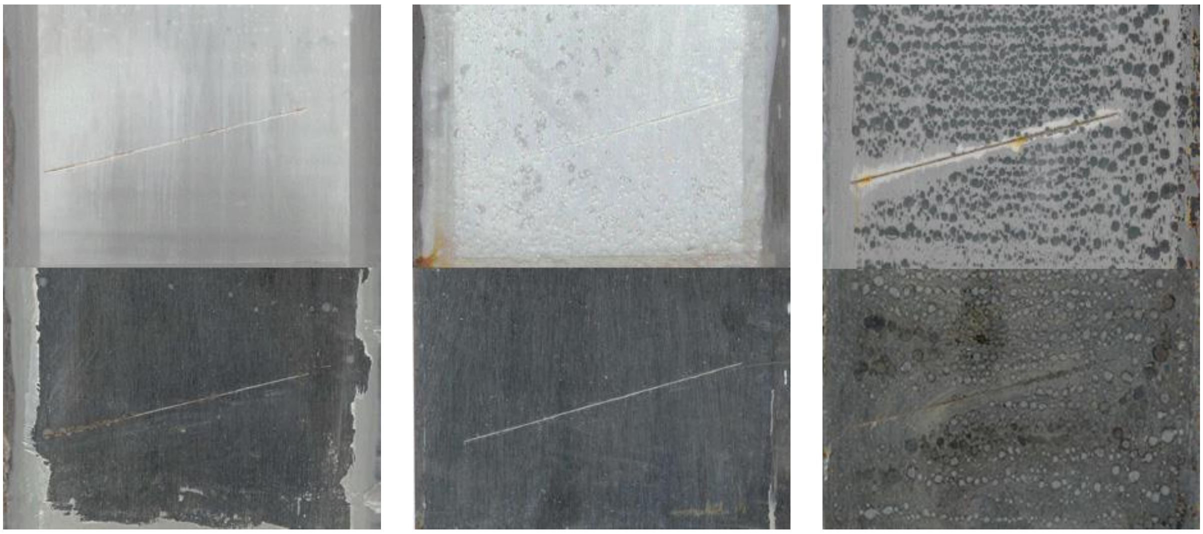

$MgMoO_4/CaSiO_3$ $MgMoO_4$. Non-pigmented film

Figure 4 Photographs of panels coated with paints containing $MgMoO_4$ or $MgMoO_4/CaSiO_3$ and exposed to the atmosphere with condensing water. In each photograph, the top part shows the condition of the paint film, and the bottom part shows the condition of the substrate metal after removing the coating.

a) Reference anticorrosion pigment

b) $ZnMoO_4$

c) MoO_3

Figure 5 Photographs of panels coated with selected paints and exposed to an atmosphere with NaCl mist. In each photograph, the top part shows the condition of the paint film, while the bottom part shows the condition of the substrate metal after removing the coating.

Table I Results of structure analysis of the pigments, identification of the phases observed

Pigment phase identified	Pigment formula (used here)	Lattice type
Stoichiometric molybdates		
Zinc Molybdenum Oxide	$ZnMoO_4$	Triclinic
Powellite, Molybdenite	$CaMoO_4$, MoO_3	Tetragonal, orthorhombic
Stroncium Molybdenum Oxide	$SrMoO_4$	Tetragonal
Magnesium Molybdenum Oxide, Molybdenum Oxide	$MgMoO_4$, Mo_4O_{11}	Monoclinic, monoclinic
Iron Molybdenum Oxide	$Fe_2(MoO_4)_3$	Monoclinic
Core-shell molybdates		
Powellite[1], Wollastonite, $CaMoO_4$, $CaSiO_3$	$ZnMoO_4$/ $CaSiO_3$	Tetragonal, monoclinic
Powellite, Wollastonite, $CaMoO_4$, $CaSiO_3$	$CaMoO_4$/ $CaSiO_3$	Tetragonal, monoclinic
Powellite[2], Wollastonite, $CaMoO_4$, $CaSiO_3$	$SrMoO_4$/ $CaSiO_3$	Tetragonal, monoclinic
Powellite[3], Wollastonite, Quartz, $CaMoO_4$ $CaSiO_3$, SiO_2	$MgMoO_4$/ $CaSiO_3$	Tetragonal, monoclinic hexagonal
Powellite[4], Wollastonite, $CaMoO_4$, $CaSiO_3$	$Fe_2(MoO_4)_3$ / $CaSiO_3$	Tetragonal, monoclinic
Powellite, Calcite[5] $CaMoO_4$, $CaCO_3$- Molybdenite[6]	Reference pigment MoO_3	Tetragonal, hexagonal Orthorhombic

Explanatory: [1] Zn ions substituted isomorphically Ca ions in the crystal lattice; [2] Sr ions substituted isomorphically Ca ions in the crystal lattice; [3] Mg ions substituted isomorphically Ca ions in the crystal lattice; [4] Fe ions substituted isomorphically Ca ions in the crystal lattice; [5] Reference pigment; [6] Starting substance, MoO_3.

Table II Physico-chemical properties of the molybdate pigments

Pigment	Density [g/cm^3]	Oil consumption [g/100g pigment]	W_{100} [%]	W_{20} [%]	pH [-]	Specific electric conductivity [µS/cm]	CPVC [-]
Stoichiometric molybdates							
$ZnMoO_4$	3.108	31.46	1.429	0.828	5.3	1861	49
$CaMoO_4$	4.231	15.50	1.001	0.398	4.7	580	59
$SrMoO_4$	4.739	13.88	0.757	0.675	4.6	221	57
$MgMoO_4$	3,804	13.93	1.792	1.644	6.3	2810	64
$Fe_2(MoO_4)_3$	3.734	20.99	0.677	0.532	4.5	176	54
Core-shell molybdates							
$ZnMoO_4/CaSiO_3$	3,072	27.41	0.934	0.754	11.8	890	52
$CaMoO_4/CaSiO_3$	3.050	29.06	2.723	1.804	12.3	6960	51
$SrMoO_4/CaSiO_3$	3,035	33.95	3.038	1.915	12.2	6620	47
$MgMoO_4/CaSiO_3$	3.066	30.86	1.376	0.664	12.1	1840	50
$Fe_2(MoO_4)_3/CaSiO_3$	3.051	28.17	0.582	0.546	11.0	270	51
Reference pigment	3.171	25.47	0.350	0.224	8.6	150	54
MoO_3	4.550	14.42	0.944	0.851	2.6	86	59

Table III Steel corrosion losses in aqueous extracts of the pigments and the pH and specific conductivity levels at the beginning and at the end of the test

Pigment	X_{corr} [%]	**pH**		**Specific electric conductivity [µS/cm]**	
		pH_1 Day 1	**pH_{21} Day 21**	**χ_1 Day 1**	**χ_{21} Day 21**
Stoichiometric molybdates					
$ZnMoO_4$	64.03	5.6	5.7	2030	1989
$CaMoO_4$	71.48	5.5	5.7	687	596
$SrMoO_4$	43.93	5.2	5.5	326	270
$MgMoO_4$	59.17	6.4	6.4	2700	2810
$Fe_2(MoO_4)_3$	45.10	5.6	5.9	285	270
Core-shell molybdates					
$ZnMoO_4/CaSiO_3$	66.38	11.5	11.2	790	500
$CaMoO_4/CaSiO_3$	78.77	12.4	12.2	6250	5990
$SrMoO_4/CaSiO_3$	45.14	12.2	12.1	6230	5500
$MgMoO_4/CaSiO_3$	46.85	11.8	11.5	1700	1105
$Fe_2(MoO_4)_3/CaSiO_3$	42.53	10.7	10.3	201	180
Reference anticorrosion pigment, reference experiments					
Reference pigment	71.37	8.2	7.1	158	140
MoO_3	70.73	5.2	5.4	533	311
Water	71.23	7.1	8.1	13	15

Table IV Results of the paint corrosion tests in the presence of SO_2 (DFT = 85 ± 15 µm)

Pigment	**Blisters in the paint film**		**Substrate metal corrosion**		**Corrosion in the cut**		**Overall anticorrosion efficiency E_{SO2}**
	ASTM D 714-87	**Score**	**ASTM D 610 [%]**	**Score**	**ASTM D 1654-92**	Score	
Stoichiometric molybdates							
$ZnMoO_4$	6F	70	0.1	95	3 - 5	50	72
$CaMoO_4$	4F	65	33	20	> 16	0	28
$SrMoO_4$	6F	70	3	70	5 - 7	40	60
$MgMoO_4$	-	100	10	60	> 16	0	53
$Fe_2(MoO_4)$	-	100	-	100	2 - 3	60	87
Core-shell molybdates							
$ZnMoO_4$/ $CaSiO_3$	-	100	-	100	> 16	0	67
$CaMoO_4$/ $CaSiO_3$	6M	50	0.03	100	7 - 10	30	60
$SrMoO_4$/ $CaSiO_3$	-	100	0.1	95	5 - 7	40	78
$MgMoO_4$/ $CaSiO_3$	-	100	-	100	7 - 10	30	77
$Fe_2MoO_4)_3/CaSiO_3$	-	100	-	100	2 - 3	60	87
Reference anticorrosion pigment, reference experiments							
Reference pigment	-	100	0.1	95	3 - 5	50	82
MoO_3	-	100	16	40	0.5 - 1	80	73
Non-pigmented film	4F	65	50	0	10 - 13	20	28

Table V Results of the paint corrosion tests in the environment with condensing water (DFT = 80 ± 15 µm)

Pigment	**Blisters on the paint film**		**Substrate metal corrosion**		**Corrosion in the cut**		**Overall anticorrosion efficiency E_{H2O}**
	ASTM D 714-87	**Score**	**ASTM D 610 hh**	**Score**	**ASTM D 1654-92**	**Score**	
Stoichiometric molybdates							
$ZnMoO_4$	8F	75	-	100	-	95	90
$CaMoO_4$	-	100	-	100	-	95	98
$SrMoO_4$	2MD	20	33	20	3 - 5	50	30
$MgMoO_4$	-	100	-	100	-	95	98
$Fe_2(MoO_4)$	-	100	-	100	-	95	98
Core-shell molybdates							
$ZnMoO_4/CaSiO_3$	4MD	25	3	70	5 - 7	40	45
$CaMoO_4/CaSiO_3$	6M	50	0.3	90	3 - 5	50	63
$SrMoO_4/ CaSiO_3$	2MD	20	0.3	90	5 - 7	40	50
$MgMoO_4/CaSiO_3$	6M	50	1	80	1 - 2	70	67
$Fe_2(MoO_4)_3/CaSiO_3$	6M	50	1	80	0.5 - 1	80	70
Reference anticorrosion pigment, starting MoO_3, reference experiments							
Reference pigment	4M	45	10	60	2 - 3	60	55
MoO_3	4MD	25	-	100	1 - 2	70	65
Non-pigmented film	4MD	25	50	0	1 - 2	70	32

Table VI Results of the paint corrosion tests in the salt mist environment (DFT = 80 ± 15 µm)

Pigment	Blisters on the paint film		Substrate metal corrosion		Corrosion in the cut		Overall anticorrosion efficiency E_{NaCl} [-]
	ASTM D 714-87	Score	ASTM D 610	Score	ASTM D 1654-92	Score	
Stoichiometric molybdates							
$ZnMoO_4$	2F	60	-	100	2 - 3	60	73
$CaMoO_4$	4F	65	50	0	10 - 13	20	28
$SrMoO_4$	2M	40	0.1	95	13 - 16	10	48
$MgMoO_4$	4M	45	0,1	95	13 - 16	10	50
$Fe_2(MoO_4)_3$	-	100	-	100	5 - 7	40	80
Core-shell molybdates							
$ZnMoO_4$/ $CaSiO_3$	-	100	-	100	5 - 7	40	80
$CaMoO_4/CaSiO_3$	6F	70	0,1	95	13 - 16	10	58
$SrMoO_4/CaSiO_3$	-	100	0.1	95	5 - 7	40	78
$MgMoO_4/CaSiO_3$	-	100	-	100	3 - 5	50	83
$Fe_2(MoO_4)_3/CaSiO_3$	-	100	0,1	95	5 - 7	40	78
Reference pigment, starting substance, blank							
Reference pigment	4F	65	0,3	90	10 - 13	20	58
MoO_3	2D	0	50	0	0.5 - 1	80	27
Non-pigmented film	4M	45	33	20	5 - 7	40	35

Table VII Data of surface hardness and adhesion of the paint films (DFT = 60 ± 10 µm)

Pigment present in the paint	**Day**									**Degree of adhesion**
	1	**2**	**3**	**8**	**15**	**28**	**43**	**78**	**112**	
Stoichiometric molybdate										
$ZnMoO_4$	9.4	14.0	19.1	25,9	29.3	29.0	36.3	39.2	41,4	0
$CaMoO_4$	9.4	15.4	29.1	38.	44.4	4.8	47.5	47.9	48.4	1
$SrMoO_4$	24,1	38.1	43.9	52.2	56.6	58.2	58.1	58.3	58.3	1
$MgMoO_4$	13.6	21.4	28.6	39.4	40,6	38.9	47,5	49.9	50.7	1
$Fe_2(MoO_4)_3$	9.9	17.1	21.1	27.3	29.6	29.7	36.4	39,9	40.5	0
Core-shell molybdates										
$ZnMoO_4/CaSiO_3$	20.7	31.6	35.6	47.1	51.8	52.9	59.0	61.0	61.3	0
$CaMoO_4/CaSiO_3$	18.6	29.4	36.6	48.5	52.9	54.0	59.9	63.2	63.5	0
$SrMoO_4/CaSiO_3$	22.8	32.6	38.2	47.9	55.5	55.6	55.7	56.9	57.8	0
$MgMoO_4/CaSiO_3$	20.6	32.7	36.9	47.9	50.4	52.2	59.1	60.2	61,4	1
$Fe_2(MoO_4)_3/CaSiO_3$	24.1	33.5	34.9	46.1	49.1	50.8	56.1	62.2	62.3	0
Reference anticorrosion pigment, starting MoO_3, non-pigmented coating material										
Reference anticorrosion pigment	9.9	17,1	21.3	30.4	34.4	35,8	36,7	36,3	36,6	0
MoO_3	4.4	5,2	6.0	6.8	7.8	9,5	10,8	12,9	13,8	1
Non-pigmented film	21.5	36.3	47.2	53.0	53.0	54,2	59,4	60,8	61,6	0